


PAPER

Cite this: *Anal. Methods*, 2023, 15, 1674

Ultra-repeatability measurement of calorific value of coal by NIRS-XRF

Rui Gao,^{ab} Jiakuan Li,^{ab} Shuqing Wang,^c Yan Zhang,^d Lei Zhang,^e ^{*ab} Zefu Ye,^e Zhujun Zhu,^e Wangbao Yin^{*ab} and Suotang Jia^{ab}

Calorific value is an important indicator to evaluate the comprehensive quality of coal, and its real-time and rapid analysis is of great significance for optimizing the coal blending process and improving boiler combustion efficiency. Traditional assays are time-consuming, and prompt gamma neutron activation analysis (PGNAA) and laser-induced breakdown spectroscopy (LIBS) have certain limitations. In this paper, a novel technique for ultra-repeatability measurement of coal calorific value by combining near-infrared spectroscopy (NIRS) and X-ray fluorescence (XRF) is proposed. In this NIRS-XRF technology, the former can stably measure organic components such as C–H and N–H that are positively correlated with the calorific value, while the latter can stably measure inorganic elements such as Na, Al, Si, Ca, Fe, and Mn that are negatively correlated with the calorific value. The combination of the two can greatly improve the measurement repeatability of coal calorific value. In the quantitative analysis algorithm, a holistic-segmented prediction model based on partial least squares (PLS) is proposed, that is, the holistic model is used to roughly predict the calorific value and determine the segment accordingly, and then the corresponding segmented model is used to accurately predict the calorific value. The experimental results show that the root mean square error of prediction (RMSEP), the average relative error (ARE), and the standard deviation (SD) of this method for predicting the calorific value of coal are 0.71 MJ kg⁻¹, 1.18% and 0.07 MJ kg⁻¹ respectively. The measurement repeatability meets the requirements of the Chinese national standard. This calorific value measurement technology based on NIRS-XRF is safe, fast, and stable, providing a new way to optimize and control the utilization process of coal in coal washing plants, power plants, coking, and other industries.

Received 25th December 2022

Accepted 28th February 2023

DOI: 10.1039/d2ay02086f

rsc.li/methods

1 Introduction

China is the largest producer and consumer of coal in the world, accounting for more than 60% of its total primary energy consumption for a long time. In 2021, the output of raw coal reached 4.07 billion tons, an increase of 4.7% over the previous year. Thermal power generation relying on coal combustion is the main source of power in China, with the total installed capacity accounting for 71.13% and the consumption of power coal accounting for 60%. In the coming decades, coal will still occupy the dominant position of resources.¹ Coal-fired power generation uses the heat generated by coal combustion to vaporize water, and the high-pressure steam pushes the steam engine to run, thus driving the engine to generate electricity. The better the coal

quality is, the more electricity will be produced, and the more significant the economic benefits will be. Calorific value is the main basis for determining the price of coal and is often used to calculate the heat balance of boiler combustion, thermal efficiency, and coal consumption rate of power supply.² If the calorific value is too high, the furnace is prone to slag, otherwise, the combustion may be insufficient or even fire extinguishing accidents may occur. In general, as an important indicator for evaluating coal quality,³ calorific value has important guiding significance for coal trading, coal blending, combustion, *etc.*

At present, the oxygen bomb calorimeter method specified in the national standard is mainly used to measure the calorific value of coal, that is, a certain amount of coal is put into a bomb filled with excessive oxygen for complete combustion, and then the calorific value is obtained through the temperature rise of the system. However, this method is tedious and time-consuming, which cannot enable the power plant to adjust the combustion parameters in time according to the calorific values, nor can it meet the requirements of clean and efficient production. The existing rapid analysis method of coal quality is mainly the prompt gamma neutron activation analysis (PGNAA),⁴ which uses a neutron beam to activate coal to produce high-energy prompt γ -

^aState Key Laboratory of Quantum Optics and Quantum Optics Devices, Institute of Laser Spectroscopy, Shanxi University, Taiyuan, China. E-mail: k1226@sxu.edu.cn; ywb65@sxu.edu.cn

^bCollaborative Innovation Center of Extreme Optics, Shanxi University, Taiyuan, China

^cSINOPEC Research Institute of Petroleum Processing Co., Ltd, Beijing, China

^dSchool of Optoelectronic Engineering, Xi'an Technological University, Xian, China

^eShanxi Gemeng US-China Clean Energy R&D Center Co., Ltd, Taiyuan, China

rays, and then the calorific value of coal can be obtained through energy spectrum analysis. However, this method has radioactive hazards and is difficult to be widely used by power plants. Laser-induced breakdown spectroscopy (LIBS) is a method that uses a high-energy pulsed laser to ablate the sample surface to generate high-temperature plasmas.⁵ The excited atoms and ions in the plasma will radiate photons of specific wavelengths when they transit from the higher energy state to the lower energy state. By measuring the intensity of the characteristic spectral lines, the elements in coal can be quantitatively analyzed and the calorific value can be predicted. For example, Wang⁶ *et al.* investigated the intensity and stability of C and H lines in LIBS spectra that are highly related to the calorific value of coal in the atmosphere, helium and argon respectively, and conducted the quantitative analysis using partial least squares (PLS), and found that the signal to noise ratio as well as the prediction accuracy were the best in argon. Yao⁷ *et al.* used artificial neural networks and genetic algorithm to analyze the LIBS spectra of pulverized coal, and the average absolute error and standard deviation of calorific value were 0.48 MJ kg⁻¹ and 0.86 MJ kg⁻¹, respectively. Although LIBS has great potential in online analysis and remote detection, its measurement repeatability is difficult to be further improved due to the laser pulse energy fluctuation, Rayleigh–Taylor instability, self-absorption effects, *etc.*^{8–10} Other commonly used methods for rapid spectroscopic analysis of coal quality include near-infrared spectroscopy (NIRS)¹¹ and X-ray fluorescence (XRF),¹² which are introduced below.

NIRS is an absorption spectroscopy technique based on near-infrared diffuse reflection, with a wavelength of 780–2526 nm. The spectral absorption in NIRS originates from the overtones of hydrogen-containing groups' stretching vibrations such as O–H, N–H, C–H, and S–H, as well as from stretching–bending combination involving these groups,^{13,14} so it can reflect the composition and structural information of organic substances in the sample. When near-infrared light is irradiated onto the coal, photons of different wavelengths will be selectively absorbed. According to Beer–Lambert's law,¹⁵ the absorbance of diffuse reflection is related to the amount of absorbed substances, thus the content of organic matter in coal can be determined. NIRS has been applied in the field of coal quality analysis in recent years due to its fast measurement speed, simple sample preparation, no damage to sample, simultaneous determination of multiple components, and strong anti-interference ability. For example, Bona¹⁶ *et al.* and Andrés^{17,18} *et al.* established the relationship between NIRS spectra and coal properties using PLS regression cluster analysis, and the results showed that the absolute measurement errors of properties related to the organic matter in some clusters, such as volatile matter, fixed carbon and calorific value, were 1–3%. Liu¹⁹ *et al.* used the particle swarm algorithm optimized extreme learning machine to analyze the NIRS spectra of coal, and the normalized root mean square error of prediction (RMSEP) of the calorific value was 0.026 MJ kg⁻¹. Begum²⁰ *et al.* established regression models using multiple linear regression based on the approximate data and reflectance data of NIRS spectra respectively and confirmed that the RMSEP of the former for measuring coal calorific value was 0.66 MJ kg⁻¹ lower than that

of the latter. Kim²¹ *et al.* selected the most useful near-infrared band for determining the coal properties and established prediction models for carbon, hydrogen, volatile matter and calorific value respectively by using multiple regression, and the measurement accuracy met the requirements. Although NIRS has high enough measurement repeatability, it can only be limited to the analysis of organic components in coal.

The principle of XRF is based on the excitation of atoms in the sample. The primary X-ray hits an inner shell electron of the atom and ejects it from the atom so that the open position is filled by an electron from a further outer shell and secondary X-ray fluorescence radiation is emitted. Each element will radiate characteristic X-rays of specific wavelength or energy,²² and according to Mosley's law, the wavelength or energy is related to the atomic number of the element, so quantitative analysis can be completed by detecting the intensity of characteristic X-rays.²³ XRF has been widely used in coal analysis due to its fast measurement speed and good stability. For example, Wawrzonek²⁴ *et al.* used multiple linear regression to confirm that the intensity of K_α lines of Si and Ca in XRF spectrum and the backscattering intensity have the best correlation with ash content. Tiwari²⁵ *et al.* analyzed Na, K, Si, Al, Ca, Mg, Zn, Fe, Mn and other elements in coal, fly ash and slag of various coal-fired power plants in India and optimized the voltage and current of the X-ray tube. Shimizu²⁶ *et al.* measured Cr, As and Se in bituminous coal samples from coal-fired power plants using an energy-dispersive XRF analyzer, and improved the measurement accuracy by optimizing the peaks and baselines of XRF spectra. Vincze²⁷ *et al.* carried out XRF quantitative analysis on pulverized coal from different power plants in Hungary based on iterative Monte Carlo simulation and determined the composition of major, minor and trace elements in coal. However, the detection limit of energy dispersive XRF for light elements is relatively high, and it can only detect elements with atomic numbers greater than 11 (sodium),^{28,29} so it is suitable for quantitative analysis of inorganic components in coal.³⁰

In summary, a single NIRS or XRF can be used to analyze the organic or inorganic components in coal respectively, but the calorific value is not only positively correlated with the organic content in coal, but also negatively correlated with the inorganic content.^{31,32} In this work, we carried out the experiment of combining NIRS and XRF to quantitatively analyze the calorific value of coal, and focused on exploring the spectral preprocessing and modeling methods to verify the feasibility of NIRS-XRF for high repeatability measurement of coal calorific value.

2 Experiment

The experimental NIRS-XRF setup for coal analysis is shown in Fig. 1. It is mainly composed of an NIRS module, XRF module, sample transport module, and control module, which are described below.

2.1 NIRS module

This module mainly consists of the near-infrared source, near-infrared spectrometer, optical fiber, fiber-optic probe,

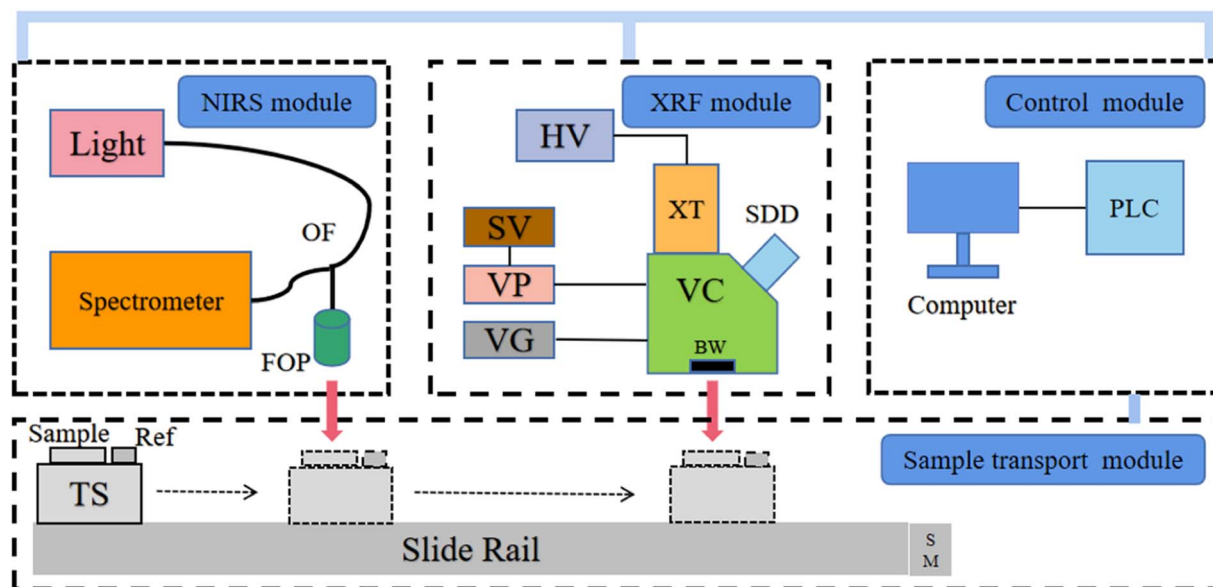


Fig. 1 Experimental NIRS-XRF setup for coal analysis (OF: optical fiber, FOP: fiber-optic probe, Ref: reference tile, VC: vacuum chamber, VP: vacuum pump, VG: vacuum gauge, SV: solenoid valve, XT: X-ray tube, HV: high-voltage power supply, BW: beryllium window, SDD: silicon drift detector, TS: translation stage, SM: stepper motor, PLC: programmable logic controller).

reference tile, *etc.* Here, the near-infrared source is a tungsten halogen lamp (AvaLight-HAL-S-Mini, Avantes) with a wavelength range of 360–2500 nm and a working life of 4000 hours. The spectrometer is a Fourier transform near-infrared (FTIR) spectrometer (C15511-01, Hamamatsu) with a spectral range of 1100–2500 nm, resolution of 5.7 nm and gain coefficient of 3. The fiber-optic probe (FCR-UVIR400-2-ME, Avantes) contains seven cores, six of which are enclosed in a circle and connected to the light source for illumination, and the remaining one is connected to the spectrometer for detection. The probe is perpendicular to the sample surface, and the spectrometer outputs the spectral data to the computer for further processing. The reference tile (WS-2, Avantes) is placed in front of the sample to facilitate the calculation of absorbance in each measurement. In the experiment, each coal sample was scanned 4096 times repeatedly, and the average of 4096 spectra collected was taken as its NIRS spectrum.

2.2 XRF module

This module is an energy-dispersive XRF, mainly composed of a vacuum chamber, vacuum pump, vacuum gauge, solenoid valve, X-ray tube, high-voltage power supply, beryllium window, silicon drift detector (SDD), *etc.* In the X-ray tube (VARIAN), the high voltage generated by the high voltage power supply (SPELLMAN) is applied between the filament and the target. The electrons emitted by the filament are accelerated by the electric field and collide with the anode target to generate X-ray, which is used as the radiation source to excite the sample. The X-ray passes through the beryllium window at the bottom of the chamber and radiates on the coal sample, which excites the secondary X-ray (*i.e.*, X-ray fluorescence) and is detected by the SDD (KETEK). The measured energy spectra are then

quantitatively analyzed by the computer. Here, the vacuum pump (VRD-8) is used to vacuum the chamber, the vacuum gauge (APG-500C) is used to monitor the atmospheric pressure inside the chamber, and the solenoid valve (VX214BAXB) is connected to the vacuum pump. In the experiment, the voltage and current of the X-ray tube were set to 16 kV and 0.6 mA respectively, while those of the filament were set to 1.5 V and 2.5 A respectively. The time constant of SDD was 2 μs , the flow rate of the vacuum pump was 2 L s^{-1} , and the air pressure in the chamber was 100 Pa. It is worth noting that the output power of the X-ray tube is easily affected by temperature, so the room temperature was always kept at 298 K.

2.3 Sample transport module

This module is used to initialize the position and transfer samples between optical modules, and is mainly comprised of a slide rail, translation stage, sample cell, stepper motor, *etc.* The size of the sample cell is 120 mm \times 20 mm \times 3 mm, with a capacity of 9 g of pulverized coal, which is fixed on the translation stage and moves on the 600 mm long slide rail. In the experiment, the sample first moved to the NIRS module at a speed of 20 mm s^{-1} and stays under it for 15 s, then moved to the XRF module at the same speed and stayed under it for 40 s, and finally returned to the initial position at a speed of 30 mm s^{-1} . It takes 80 seconds to complete the measurement of a coal sample. Note that the powder in the sample cell should be scraped smoothly before measurement to ensure the homogeneity and flatness of the surface.

2.4 Control module

This module is mainly composed of a PLC and computer. The former is used to control the working sequence of the other

modules, as well as the translation stage, vacuum pump, high-voltage power supply, solenoid valve, *etc.*, while the latter is used for spectral analysis.

2.5 Samples

A total of 344 coal samples were collected from Shanxi Duanshi coal preparation plant in China, including four types of coal, namely clean coal, medium coal, slime and gangue. After pretreatment such as crushing, screening, mixing, shrinking and air drying, these raw coals were made into air-dried pulverized coal with an average particle size of 0.2 mm. Moreover, the calorific values were certified by the national standard method. In the experiment, 316 samples were used as the calibration set to establish the prediction model of calorific value, and the remaining 28 samples were used as the validation set to evaluate the accuracy and stability of the model. Fig. 2 shows the calorific value distribution of the two sets, from which it can be seen that the total range is 1–34 MJ kg⁻¹, and the distribution is relatively uniform. Moreover, both sets include all four types of coal, which are representative. According to the calorific value, it can be classified as clean coal, medium coal, slime and gangue, even if their boundaries overlap slightly. To verify the stability of the prediction model, five coal samples were selected from the validation set for five repeated measurements to calculate the standard deviation of the prediction results.

3 Model evaluation

The correlation coefficient (R^2), RMSEP and ARE used to evaluate the accuracy and repeatability of the prediction model are as follows:

$$R^2 = 1 - \frac{\sum_{i=1}^m (y_{ai} - y_{bi})^2}{\sum_{i=1}^m (y_{ai} - \bar{y})^2}, \quad (1)$$

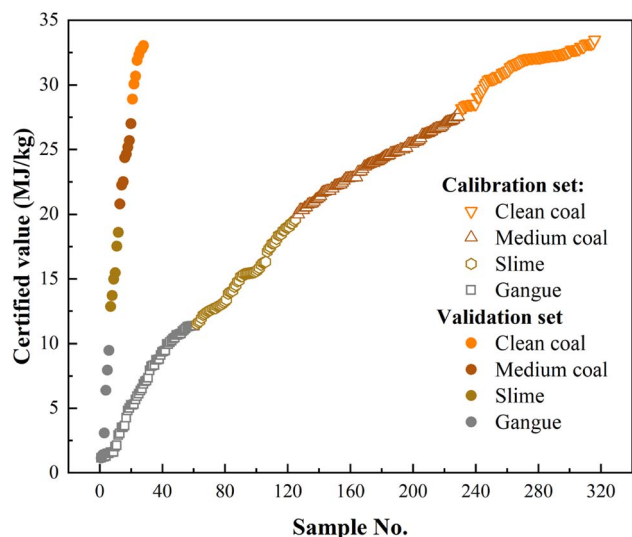


Fig. 2 Calorific value distribution of coal samples in the calibration set and validation set.

$$\text{RMSEP} = \sqrt{\frac{\sum_{i=1}^n (y_{ci} - y_{di})^2}{n}}, \quad (2)$$

$$\text{ARE} = \frac{1}{n} \sum_{i=1}^n \frac{|y_{ci} - y_{di}|}{y_{ci}} \times 100\%, \quad (3)$$

where y_a and y_b are respectively the certified and predicted calorific values of the sample in the calibration set, y_c and y_d are respectively the certified and predicted calorific values of the sample in the validation set, \bar{y} represents the average of the certified calorific value of the samples in the calibration set, i is the sample number, and m and n are the number of samples in the calibration set and validation set, respectively. The closer R^2 is to 1, the better the correlation of the prediction model is, and the closer the predicted value is to the certified value. The closer RMSEP and ARE are to 0, the smaller the deviation between the predicted value and the certified value, and the higher the prediction accuracy of the prediction model.

Here, the standard deviation (SD) is used to evaluate the measurement repeatability of the prediction model by calculating the dispersion of repeated measurement data of the same sample:

$$\text{SD} = \sqrt{\frac{\sum_{q=1}^p (V_q - V_k)^2}{p - 1}}, \quad (4)$$

where p is the total measurement times of the same coal sample, V_q is the calorific value measured for the q -th time of the same coal sample, and V_k is the mean calorific value of the same coal sample repeatedly measured for p times. The smaller the SD, the better the repeatability of the prediction model for calorific value measurement.

4 Results and discussion

4.1 Spectral pretreatment

Fig. 3 shows the comparison of typical NIRS spectra of the four types of coal in the 1100–2500 nm band obtained in the experiment, where the horizontal axis and vertical axis represent wavelength and absorbance respectively. The absorbance here is calculated from the logarithm of the ratio of the measured NIRS spectra of the coal sample to that of the reference tile, reflecting the absorption degree of the samples to near-infrared radiation at different wavelengths. It can be seen that the difference between NIRS spectra of different types of coal is obvious. Clean coal has the highest absorbance, followed by medium coal and slime, while gangue has the lowest absorbance. The absorbance of all coals basically shows a downward trend with the wavelength, and the descending gradient of the spectrum of coal slime is the smallest. The bands of 1780–1920 nm, 2100–2218 nm and 2350–2480 nm are also marked with dotted lines in the figure, representing the combination of a free water binding band, C–H stretch or C–C stretch, CH₃, CH₂ asymmetric stretch and symmetric bond respectively.

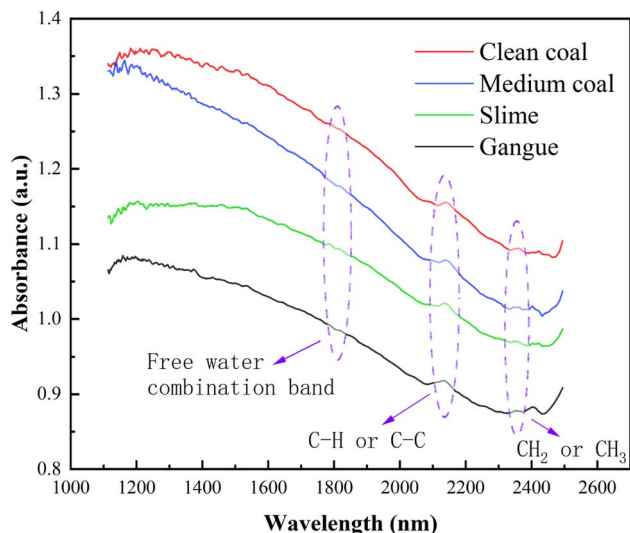


Fig. 3 Typical NIRS spectra of the four types of coal.

Fig. 4 shows typical XRF spectra of the four types of coal, in which emission lines of Na, Al, Si, S, K, Ca, Ti, Cr, Mn, Fe, Co and Cu are marked. It can be seen that the elemental components of these coals are the same, and the main difference lies in the intensity of the spectral lines. In general, the intensities of Si and Al lines in gangue are the strongest, followed by those in slime and medium coal, and the clean coal is the weakest. In addition, the low intensity of Na line is mainly due to the relatively poor excitation effect of XRF on light elements.

Due to the changes in ambient temperature and humidity, the particle size distribution of the sample, flatness of the sample surface, mechanical vibration, irradiation power, *etc.*, the background noise of NIRS and XRF spectra will increase or baselines will drift, resulting in distortion of the extracted spectral information and affecting the quantitative analysis results. Therefore, it is necessary to preprocess the raw spectra to remove irrelevant variables and improve the signal-to-noise

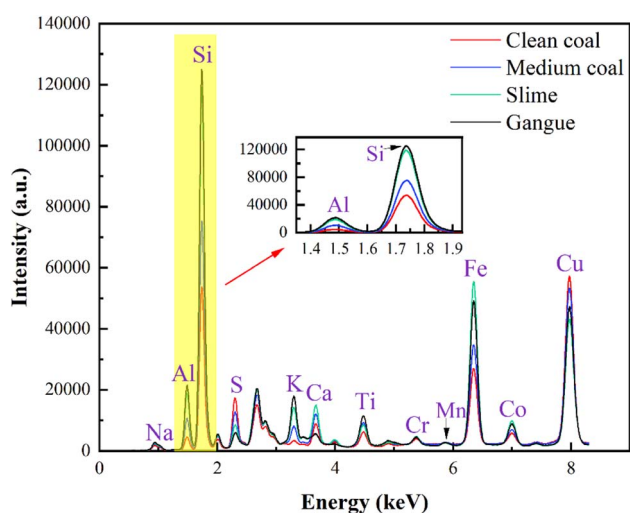


Fig. 4 Typical XRF spectra of four types of coal.

ratio. We used Savitzky–Golay convolutional smoothing algorithm to remove spectral noise, which is a filtering method based on local least-squares fitting of the data by polynomials. The so-called polynomial smoothing here is to fit the data at the moderately spaced wavelength points ($N = 2m + 1$) of the window into a polynomial model of order m , and then replace the value at the central wavelength point with the fitted smoothing value. The window is sequentially moved until the spectrum is smoothed. In this work, the window size was set to 5, and the five equally spaced points X_{m-2} , X_{m-1} , X_m , X_{m+1} , and X_{m+2} in the window were fitted with the following quadratic polynomial:

$$y = a_0 + a_1x + a_2x^2 \quad (5)$$

The standard normal variation (SNV) can eliminate the influence of scattering on the NIRS spectrum caused by coal heterogeneity, particle size difference and scattering caused by optical path variation on NIRS spectra. Compared with normalization, SNV processes not columns but rows of spectral data. Here, the calculation formula of SNV for NIRS spectra correction and denoising is:

$$X_{\text{SNV}} = \frac{x_i - \bar{x}}{\sqrt{\frac{\sum_{i=1}^n (x_i - \bar{x})^2}{n - 1}}} \quad (6)$$

where X_{SNV} denotes the spectral data of the coal sample after SNV transformation, x_i denotes the data of the i -th point in the spectrum, \bar{x} denotes the mean spectral data, and n denotes the total number of points.

4.2 Prediction model

The pretreated NIRS spectrum and XRF spectrum were connected end to end and used as the input variables of the prediction model. In the study, PLS was used to establish the quantitative prediction model of calorific value.

First, we used all the coal samples in the calibration set to establish a prediction model of calorific value, which is called the holistic model. Then, according to the characteristics of the calorific value distribution of coal, we divided it into four segments for modeling, which is called the segmented model. The quantitative analysis process is to use the holistic model to roughly predict the calorific value of the unknown sample and determine its segment, and then use the corresponding segmented model to accurately predict the calorific value.

Fig. 5 shows the comparison between the predicted calorific values of both calibration (blue circle) and validation (red circle) sets using the holistic model and the certified values. It can be seen that the R^2 of the fitting curve of the calibration set is 0.998, while the RMSEP and ARE of the validation set are 1.75 MJ kg^{-1} and 4.89%, respectively.

Due to a large number of samples in the calibration set, obvious matrix difference and the wide distribution of the calorific value of various coals, the measurement error of directly using the holistic model was large. Therefore, it was necessary to divide the calorific value interval into multiple

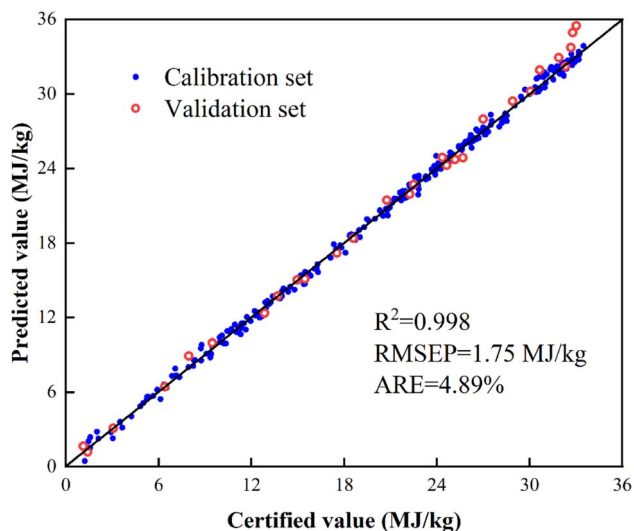


Fig. 5 Comparison between certified values and predicted values by the holistic model.

segments for modeling respectively to reduce the heterogeneity between samples and improve the measurement accuracy. The calorific value of the total sample covers 1–34 MJ kg⁻¹. Here, according to the calorific value distribution ranges of clean coal, medium coal, slime and gangue, it was divided into four segments, corresponding to 28–34 MJ kg⁻¹, 20–28 MJ kg⁻¹, 11–20 MJ kg⁻¹ and 1–11 MJ kg⁻¹ respectively. The PLS was used to obtain the four segmented models of the above segments, and the number of variables of the holistic model and the segmented models is 3739, as shown in Fig. 6. It can be seen that the R^2 values of these segmented models are higher than 0.99, and compared with the holistic model, the RMSEP of calorific value is reduced from 1.75 MJ kg⁻¹ to 0.71 MJ kg⁻¹, and ARE is reduced from 4.89% to 1.18%. These indicate that the

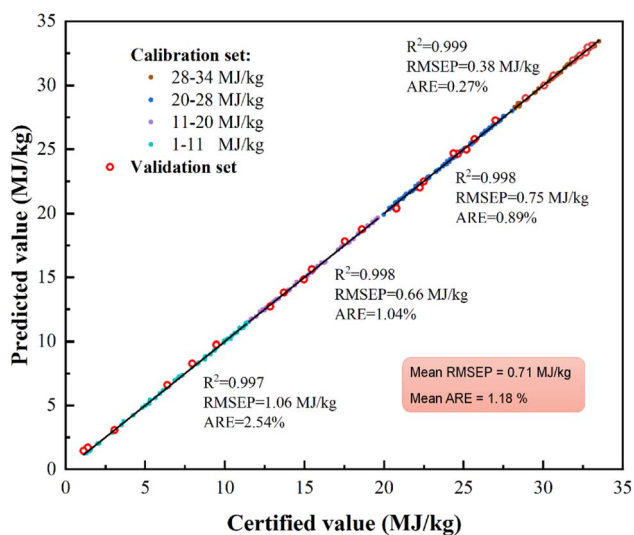


Fig. 6 Comparison between certified values and predicted values by the segmented models.

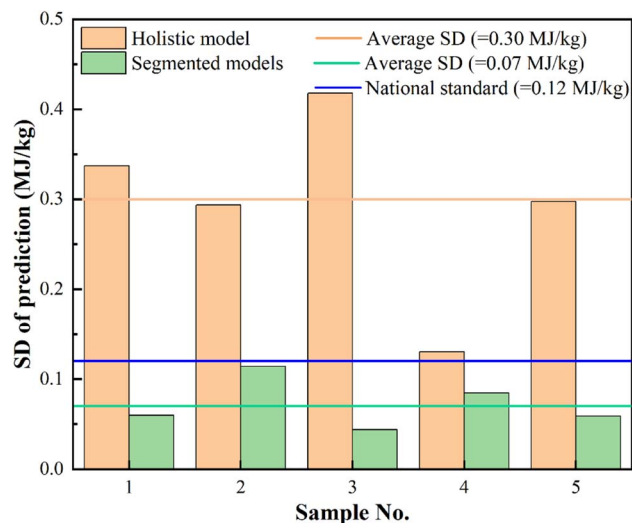


Fig. 7 Comparison between SDs of calorific values predicted by the holistic model and segmented models and national standard.

prediction results of the segmented models are indeed closer to the certified values, which can effectively improve the measurement accuracy of the calorific value.

In order to verify the repeatability of the model, one coal sample was randomly selected from clean coal, medium coal, slime, and gangue in the validation set, with a total of five samples numbered 1 to 5. Each sample was repeatedly predicted five times using the holistic model and the segmented models respectively to calculate the SDs for comparison. The results are shown in Fig. 7, where the orange line and the green line represent the mean SDs of the five coals predicted by the holistic model and the segmented models respectively, and the blue line represents the SD specified in the national standard. It can be seen that all the samples in the validation set are assigned to the correct segment with the holistic model, and the classification accuracy reaches 100%. The SDs of the segmented models are lower than those of the holistic model, and the mean SD decreases from 0.30 MJ kg⁻¹ to 0.07 MJ kg⁻¹. In addition, the mean SD of the holistic model is higher than 0.12 MJ kg⁻¹ specified in the national standard, while that of the segmented models meets this requirement. The holistic-segmented model proposed effectively solves the problem that spectral details are ignored when only the holistic model is used, and greatly improves the prediction accuracy.

5 Conclusion

In this paper, an NIRS-XRF technology for ultra-repeatability analysis of coal calorific value is proposed, which combines the advantages of NIRS and XRF that can measure organic components and inorganic elements with high stability respectively. It is not only fast, safe and nondestructive, but also does not need to make pulverized coal into tablets or generate floating dust like LIBS. For spectral analysis, a quantitative analysis algorithm based on the holistic-segmented model is adopted, that is, the holistic model is used for rough prediction

and determination of the segment, and the segmented model is used for accurate prediction. The test results show that compared with the traditional holistic model, this method reduced RMSEP from 1.75 MJ kg⁻¹ to 0.71 MJ kg⁻¹, ARE from 4.89% to 1.18%, and mean SD from 0.30 MJ kg⁻¹ to 0.07 MJ kg⁻¹. This NIRS-XRF technology combined with the quantitative analysis algorithm based on the holistic-segmented model has significantly improved the measurement accuracy of coal calorific value, while the repeatability can obviously meet the requirements of the national standard. Next, we will extend this method to quantitative analysis of other characteristics of coal, and develop a prototype for industrial field testing to verify its performance.

Author contributions

Rui Gao is the main author and is responsible for the conceptualization, methodology, software, data curation and formal analysis of the experiment, and the writing of original draft. Yan Zhang and Lei Zhang are responsible for conceptualization and methodology, while Lei Zhang is also responsible for writing review and editing, and project management. Jiaxuan Li is responsible for investigation, validation and supervision. Shuqing Wang, Zefu Ye and Zhujun Zhu are responsible for providing the necessary resources for the experiment. Wangbao Yin and Suotang Jia are responsible for project management and funding acquisition, while Wangbao Yin is also responsible for writing review and editing.

Conflicts of interest

There are no conflicts to declare.

Acknowledgements

National Key R&D Program of China (2017YFA0304203); National Energy R&D Center of Petroleum Refining Technology (RIPP, SINOPEC); Changjiang Scholars and Innovative Research Team in University of Ministry of Education of China (IRT_17R70); National Natural Science Foundation of China (NSFC) (61975103, 61875108, 627010407); 111 Project (D18001); Fund for Shanxi “1331KSC”.

References

- 1 Q. Yang, L. Zhang, S. Zou and J. Zhang, *Energy Policy*, 2020, **139**, 111360.
- 2 P. Liu and S. Lv, *Therm. Sci.*, 2020, **24**, 3129–3137.
- 3 M. Açıkkar and O. Sivrikaya, *Turk. J. Electr. Eng. Comput. Sci.*, 2018, **26**, 2541–2552.
- 4 M. Borsaru and Z. Jecny, *Appl. Radiat. Isot.*, 2001, **54**, 519–526.
- 5 W. Gu, L. Zhang, M. Dong, C. Li, Y. Tian, Z. Hou, Z. Wang and R. Zheng, *Plasma Sci. Technol.*, 2022, **24**, 4.
- 6 Z. Wang, T.-B. Yuan, S.-L. Lui, Z.-Y. Hou, X.-W. Li, Z. Li and W.-D. Ni, *Front. Phys.*, 2012, **7**, 708–713.
- 7 S. Yao, J. Mo, J. Zhao, Y. Li, X. Zhang, W. Lu and Z. Lu, *Appl. Spectrosc.*, 2018, **72**, 1225–1233.
- 8 Y. Song, W. Song, L. Li, W. Gu, K. Kou, M. S. Afgan, Z. Hou, Z. Li and Z. Wang, *Opt. Lasers Eng.*, 2023, **162**, 107433.
- 9 Y.-T. Fu, W.-L. Gu, Z.-Y. Hou, S. A. Muhammed, T.-Q. Li, Y. Wang and Z. Wang, *Front. Phys.*, 2020, **16**, 22502.
- 10 S. Sheta, M. S. Afgan, Z. Hou, S.-C. Yao, L. Zhang, Z. Li and Z. Wang, *J. Anal. At. Spectrom.*, 2019, **34**, 1047–1082.
- 11 Y. Ozaki, *Anal. Sci.*, 2012, **28**, 545–563.
- 12 V. Panchuk, I. Yaroshenko, A. Legin, V. Semenov and D. Kirsanov, *Anal. Chim. Acta*, 2018, **1040**, 19–32.
- 13 P. Duan, S. Han, W. Wang and Y. Tang, *ACS Omega*, 2022, **7**, 2023–2030.
- 14 K. B. Bec, J. Grabska and C. W. Huck, *Chemistry*, 2021, **27**, 1514–1532.
- 15 K. Fuwa and B. L. Valle, *Anal. Chem.*, 2002, **35**, 942–946.
- 16 M. T. Bona and J. M. Andres, *Talanta*, 2007, **72**, 1423–1431.
- 17 J. M. Andrés and M. T. Bona, *Anal. Chim. Acta*, 2005, **535**, 123–132.
- 18 J. M. Andres and M. T. Bona, *Talanta*, 2006, **70**, 711–719.
- 19 W. Liu, B. Peng, X. Liu, F. Ren and L. Zhang, *J. Appl. Spectrosc.*, 2021, **88**, 645–652.
- 20 N. Begum, D. Chakravarty and B. S. Das, *Int. J. Coal Prep. Util.*, 2019, **42**, 979–985.
- 21 D. W. Kim, J. M. Lee and J. S. Kim, *Korean J. Chem. Eng.*, 2009, **26**, 489–495.
- 22 P. J. Potts, A. T. Ellis, P. Kregsamer, C. Strelis, C. Vanhoof, M. West and P. Wobrauschek, *J. Anal. At. Spectrom.*, 2006, **21**, 1076–1107.
- 23 M. Chand, G. V. S. Ashok Kumar, R. Senthilvadivu, K. Usha Lakshmi, M. Serajuddin, G. Ramadevi and R. Kumar, *Appl. Radiat. Isot.*, 2022, **187**, 110336.
- 24 L. Wawrzonek and J. L. Parus, *Isot. Environ. Health Stud.*, 2008, **24**, 82–84.
- 25 M. Tiwari, S. K. Sahu, R. C. Bhangare, P. Y. Ajmal and G. G. Pandit, *Appl. Radiat. Isot.*, 2014, **90**, 53–57.
- 26 R. Shimizu, H. Masaki and S. Yasuike, *Appl. Radiat. Isot.*, 2021, **176**, 109877.
- 27 L. Vincze, A. Somogyi, J. Osan, B. Vekemans, S. Torok, K. Janssens and F. Adams, *Anal. Chem.*, 2002, **74**, 1128–1135.
- 28 J. Liu, X. Jiang, Y. Zhang, H. Zhang, L. Luo and X. Wang, *Fuel*, 2016, **181**, 1081–1088.
- 29 D. Baimonda, G. Bernasconi, N. Haselberger, A. Markowicz and V. Valkovic, *J. Radioanal. Nucl. Chem.*, 1994, **185**, 27–34.
- 30 E. Grabias-Blicharz, R. Panek, M. Franus and W. Franus, *Materials*, 2022, **15**, 7174.
- 31 X. Li, L. Zhang, Z. Tian, Y. Bai, S. Wang, J. Han, G. Xia, W. Ma, L. Dong, W. Yin, L. Xiao and S. Jia, *J. Anal. At. Spectrom.*, 2020, **35**, 2928–2934.
- 32 A. R. Shirazi, O. Börtin, L. Eklund and O. Lindqvist, *Fuel*, 1995, **74**, 247–251.